Frontiers of Information Technology & Electronic Engineering
www.jzus.zju.edu.cn; engineering.cae.cn; www.springerlink.com
ISSN 2095-9184 (print); ISSN 2095-9230 (online)
E-mail: jzus@zju.edu.cn

Trajectory Poisson multi-Bernoulli filters with unknown detection probability*

Xiangfei ZHENG[1], Kaidi LIU[1], Hongwei LI‡[1]

[1] *School of Mathematics and Physics, China University of Geosciences, Wuhan 430074, China*

E-mail: zxfdouble@cug.edu.cn; lkd1028@cug.edu.cn; hwli@cug.edu.cn

Received July 18, 2024; Revision accepted Dec. 17, 2024; Crosschecked

Abstract: Compared with general multi-target (MTT) tracking filters, this paper focuses on multi-target trajectory estimation in scenarios where the detection probability of the sensor is unknown. In this paper, two trajectory Poisson multi-Bernoulli (TPMB) filters with unknown detection probability are proposed: one for alive trajectories and the other for all trajectories. First, the augmented trajectory state with detection probability is constructed, and then two new state transition models and a new measurement model are proposed. Then, this paper derives the recursion of TPMB filters with unknown detection probability. Furthermore, the detailed beta-Gaussian (BG) implementations of TPMB filters for alive trajectories and all trajectories are presented. Finally, simulation results demonstrate that the proposed TPMB filters with unknown detection probability can achieve robust tracking performance and effectively estimate multi-target trajectories even when the detection probability is unknown.

Key words: Trajectory Poisson multi-Bernoulli; Beta-Gaussian; Detection probability; Alive trajectories; All trajectories

https://doi.org/10.1631/FITEE.2400606 **CLC number:** TP

1 Introduction

Multi-target tracking (MTT) aims to estimate the number of targets of interest in the scene as well as their position and velocity based on the measurement data containing target position, false alarm and clutter received by the sensor (Mahler, 2007, 2014). MTT is widely used in many fields, such as autonomous driving(Chen et al., 2016; Pang et al., 2021), missiles(Menegaz and Battistini, 2018; Yu et al., 2018), robotics(Gao et al., 2020), radar systems(Yan et al., 2022; Joshi et al., 2022), ship tracking(Granström et al., 2015) and so on. For MMT, common solutions include joint probabilistic data association(JPDA) (Fortmann et al., 1983), multiple hypothesis tracking(MHT)(Blackman, 2004), and random finite set (RFS) framework(Mahler, 2007, 2014). The RFS framework models both the target state and the measurement as RFSs, avoiding the data association between the target state and the measurement. Compared with JPDA and MHT, the RFS framework avoids explicit data association and reduces the algorithm complexity, which has attracted the attention of many scholars.

A series of MTT filters based on the RFS framework is proposed, mainly including probability hypothesis density (PHD) filter(Vo and Ma, 2006), cardinality PHD (CPHD) filter(Vo et al., 2007), cardinality balanced multi-target multi-Bernoulli (CBMeMBer) filter(Vo et al., 2009), δ-generalized labeled multi-Bernoulli (GLMB) filter (Vo and Vo, 2013) and LMB filter (Vo et al., 2014). The Poisson multi-Bernoulli mixture (PMBM) filter is proposed to solve the problem of undetected targets due to obstruction(García-Fernández et al., 2018; Granström et al., 2020). PMBM filter is defined as Poisson RFS

‡ Corresponding author

* Project supported by the National Natural Science Foundation of China (No. 42374174)

ORCID: Xiangfei ZHENG, https://orcid.org/0000-0001-8384-6703; Hongwei LI, https://orcid.org/0000-0001-6809-7097

and multi-Bernoulli mixture (MBM) RFS(García-Fernández et al., 2018) convolution, where Poisson RFS represents undetected targets and MBM RFS represents detected targets. Note that the PMBM filter density is given by the MBM filter when the birth model of PMBM is multi-Bernoulli (MB) instead of Poisson. When MB is used to represent detected targets, the PMBM filter density is given by the PMB filter(Xia et al., 2022). Similar to GLMB, PMBM is also a multi-target conjugate prior filter. It is important to note that the GLMB filter and LMB filter mentioned above are considered labeled filters, while the rest are considered unlabeled filters.

Filters can be either unlabeled, providing an estimate of the target set at the current time, or labeled, providing information about the target set at the current time as well as their trajectories. The GLMB filter and LMB filter add a unique label to the target state and form a trajectory by associating the target state estimate with the same label. However, the (G)LMB filter is only suitable for MB birth models and not suitable for independent identically distributed cluster birth models.(García-Fernández et al., 2020b).

To estimate the trajectory of the target, Li et al. (2019) proposed the continuous function of time to model the target trajectory, and Houssineau et al. (2021) proposed a multi-target trajectory tracking filter through the possibility theory. In addition to the above trajectory filters, García-Fernández et al. (2020b) proposed a RFS of trajectories (TRFS) that models the trajectories state as a set. TRFS can obtain the trajectory of the target without using the target's label. Then, the TRFS is extended to PMBM filter and the trajectory PMBM filter (TPMBM) is proposed by Granström et al. (2018). García-Fernández and Svensson (2019) proposed trajectory PHD (TPHD) and trajectory CPHD (TCPHD) filters. T(C)PHD reduces the storage space while maintaining accuracy by adding the track window. When the track window is L = 1, T(C)PHD degrades to (C)PHD. Gaussian implementations of trajectory Poisson multi-Bernoulli (TPMB) filters for alive trajectories and all trajectories are provided by García-Fernández et al. (2020c), where the alive trajectories represent trajectories that are still alive in the monitored area at the current time and all trajectories represent the trajectories that have been presented in the monitoring area. The Gaussian implementation of TPMB filters for alive trajectories estimates the set of alive trajectories at each time step, while the other estimates the set of all trajectories at each time step. In the TPMB filters above, the Poisson component represents undetected trajectories and the MB component represents detected trajectories. Due to the true posterior of TPMB being a TPMBM, the TPMB filter is derived by using Kullback-Leibler divergence (KLD) minimization on a trajectory space with auxiliary variables, after each update(García-Fernández et al., 2020c).

It is worth noting that the detection probabilities of all the above filters are given as prior information, and the detection probabilities of the sensors are assumed to be constant. However, in real scenarios, the detection probability of the sensor is often affected by factors such as its own hardware, external environment, and detection distance, resulting in unknown detection probability and time-varying detection probability. To overcome the impact of unknown detection probability and time variation on target tracking, Mahler used beta distribution to describe detection probability and proposed the corresponding robust (C)PHD filter and robust MB filter (Mahler et al., 2011; Vo et al., 2013). The unknown detection probability PMBM filter is proposed by Li et al. (2021), and the robust extended target PMBM filter is further implemented by Xie et al. (2023) and Wu et al. (2022). Although the above filters can achieve multi-target estimation under unknown detection probability, they can only estimate the multi-target state at the current moment. They cannot estimate the trajectory of the tracked target. To get a direct estimate of the trajectory state, Wei et al. (2022) proposed a trajectory RFS filter with unknown detection probability for the first time based on T(C)PHD filter. However, the methods in the study of Wei et al. (2022) only consider alive trajectory tracking within a track window and do not consider all trajectories tracking.

In this paper, TPMB filters with unknown detection probability are proposed to address the issue of tracking alive trajectories and all trajectories. The main contributions of this paper are as follows:

(1) This paper proposes TPMB filters that can adaptively learn the unknown detection probability while estimating the trajectories of targets. One TPMB filter aims to estimate the set of alive tra-

jectories with unknown detection probability, while the other aims to estimate the set of all trajectories with unknown detection probability. The augmented trajectory state space model is constructed for the trajectory kinematics and detection probability and propagates them by applying the TPMB filters. Moreover, the expressions of the proposed filter recursion are given.

(2) In this paper, the computationally feasible implementations of the proposed TPMB filters with unknown detection probability are proposed. First, the trajectory's state is modeled by the beta-Gaussian (BG) distribution, where the beta distribution is used to model the detection probability and the Gaussian distribution is used to model the kinematic state. Then, the closed-form solutions to the TPMB filter for alive trajectories and the TPMB filter for all trajectories are given, respectively, via BG implementation.

The rest of the paper is organized as follows. The background of multi-target trajectory tracking is introduced in Section 2. The proposed TPMB filters with unknown detection probability are presented in Section 3 and their BG implementations in Section 4. Simulation results are shown in Section 5, and conclusion is provided in Section 6.

2 Background

This section briefly reviews the TPMB filter. TRFS is given in Section 2.1, TPMBM with auxiliary variable and TPMB approximation filter are reviewed in Sections 2.2 and 2.3, respectively.

2.1 TRFS

Suppose that $x \in \mathbb{R}^{n_x}$ represents the single target state, where n_x denotes the dimension of the state x and x contains the kinematic information of the target, e.g., position and velocity of the target. Then the single trajectory state is represented as $X = \left(t, x^{1:\nu}\right)$, where t represents the initial time of the trajectory, $x^{1:\nu} = \left(x^1, x^2, \ldots, x^\nu\right)$ is a finite sequence of single target states, the sequence length is ν, and x^i, $i \in \{1, 2, \ldots, \nu\}$, denotes the state of the target at time step $t + i - 1$.

At time step k, for the trajectory $X = \left(t, x^{1:\nu}\right)$, the variable (t, ν) belongs to the set $I_k = \{(t, \nu) : 0 \le t \le k, 1 \le \nu \le k - t + 1\}$, and $X \in T_{(k)} = \uplus_{(t,\nu)\in I_k} \{t\} \times \mathbb{R}^{\nu n_x}$, where $\uplus$ denotes the union of sets that are mutually disjoint and $\times$ denotes a Cartesian product. The set of trajectories up to time k is represented as $\mathbf{X}_k = \left\{X_{k,1}, X_{k,2}, \ldots, X_{k,N_{\mathbf{X}_k}}\right\} \in \mathcal{F}\left(T_{(k)}\right)$, where $\mathcal{F}\left(T_{(k)}\right)$ is the set of all finite subsets of $T_{(k)}$ and $N_{\mathbf{X}_k}$ is the number of elements in the set of trajectories $\mathbf{X}_k$.

2.2 TPMBM with auxiliary variable

In this subsection, the TPMB approximation filter is reviewed. The TPMB approximation filter extends the single trajectory space with an auxiliary variable $u \in \mathbb{U}_k = \{0, 1, 2, \ldots, n_k\}$, such that $\tilde{X} = (u, X) \in \mathbb{U}_k \times T_{(k)}$(García-Fernández et al., 2020c). The variable $u = 0$ denotes the undetected trajectory, it corresponds to Poisson point process (PPP), and the variable $u = i$ denotes a single trajectory corresponding to the i-th Bernoulli component. The set of trajectories with an auxiliary variable $\tilde{\mathbf{X}}$ belongs to $\mathcal{F}\left(\mathbb{U}_k \times T_{(k)}\right)$. Then TPMBM with auxiliary variable density at time step k can be represented by

$$f_k(\tilde{\mathbf{X}}_k) = \sum_{\left(\uplus_{l=1}^{n_k} \tilde{\mathbf{X}}_k^l\right)\uplus \tilde{\mathbf{Y}}_k = \tilde{\mathbf{X}}_k} f_k^p(\tilde{\mathbf{Y}}_k) \times \sum_{a\in\mathcal{A}_k} w_k^a \prod_{i=1}^{n_k} \left[f_k^{i,a^i}\left(\tilde{\mathbf{X}}_k^i\right)\right], \tag{1}$$

where n_k is the number of Bernoulli component, $\tilde{\mathbf{Y}}_k = \left\{(u, X) \in \tilde{\mathbf{X}}_k : u = 0\right\}$, $\tilde{\mathbf{X}}_k^i = \left\{(u, X) \in \tilde{\mathbf{X}}_k : u = i\right\}$. $f_k^p\left(\tilde{\mathbf{X}}\right)$ is the density of Poisson RFS, representing the undetected trajectories,

$$f_k^p(\tilde{\mathbf{X}}) = e^{-\int \lambda_k(\tilde{X}) d\tilde{X}} \left[\lambda_k(\cdot)\right]^{\tilde{\mathbf{X}}}, \tag{2}$$

$$\lambda_k(\tilde{X}) = \lambda_k(u, X) = \delta_0[u]\, \lambda_k(X), \tag{3}$$

$$\delta_A[B] = \begin{cases} 1, & A = B; \\ 0, & A \ne B, \end{cases} \tag{4}$$

$f_k^{i,a^i}(\tilde{\mathbf{X}})$ is the density of Bernoulli RFS, representing the detected trajectories,

$$f_k^{i,a^i}(\tilde{\mathbf{X}}) = \begin{cases} 1 - r_k^{i,a^i}, & \tilde{\mathbf{X}} = \emptyset; \\ r_k^{i,a^i} p_k^{i,a^i}(X)\delta_i[u], & \tilde{\mathbf{X}} = \{(u, X)\}; \\ 0, & otherwise, \end{cases} \tag{5}$$

$$w_k^a = \frac{\prod_{i=1}^{n_k} w_k^{i,a^i}}{\sum_{\theta\in\mathcal{A}_k}\prod_{i=1}^{n_k} w_k^{i,\theta^i}}, \tag{6}$$

where w_k^a denotes the weight of global hypothesis a, and $a = \left(a^1, a^2, \ldots, a^{n_k}\right)$, $a^i \in \left\{1, 2, \ldots, h^i\right\}$ is the index of the local hypothesis of the i-th Bernoulli component and h^i denotes the number of local hypothesis, w_k^{i,a^i} denotes the weight of local hypothesis a^i related to the i-th Bernoulli component, $\mathcal{A}_k$ is the set of all global hypotheses.

2.3 TPMB approximation

For TPMBM density with auxiliary variable $f_k(\cdot)$ in Section 2.2, the TPMB approximation density based on minimizing the KLD is as follows(García-Fernández et al., 2020c):

$$\tilde{f}_k(\tilde{\mathbf{X}}_k) = \tilde{f}_k^p(\tilde{\mathbf{Y}}_k)\prod_{i=1}^{n_k}\left[\tilde{f}_k^{i,1}\left(\tilde{\mathbf{X}}_k^i\right)\right], \tag{7}$$

where $\tilde{f}_k^p(\tilde{\mathbf{Y}}_k)$ is given by Eq.(2), $\tilde{f}_k^i\left(\tilde{\mathbf{X}}_k^i\right)$ is given by Eq.(5) with $a^i = 1$, $i \in \{1, 2, \ldots, n_k\}$. $a^i = 1$ implies that the i-th Bernoulli component retains only one local hypothesis, which is usually omitted from the Bernoulli parameters, i.e., existence probability and trajectory density in Eq.(5) are r_k^i and $p_k^i(\cdot)$. Then,the Bernoulli parameters r_k^i and $p_k^i(\cdot)$ are given by:

$$r_k^i = \sum_{a^i=1}^{h_i} \bar{w}_k^{i,a^i} r_k^{i,a^i}, \tag{8}$$

$$p_k^i(X) = \frac{\sum_{a^i=1}^{h_i} \bar{w}_k^{i,a^i} r_k^{i,a^i} p_k^{i,a^i}(X)}{\sum_{a^i=1}^{h_i} \bar{w}_k^{i,a^i} r_k^{i,a^i}}, \tag{9}$$

where

$$\bar{w}_k^{i,a^i} = \sum_{\theta\in\mathcal{A}_k:\theta^i=a^i} w_k^{\theta}. \tag{10}$$

3 TPMB filters with unknown detection probability

Section 3.1 proposes the augmented trajectory state space model for the set of alive trajectories and the set of all trajectories. The recursions of the TPMB filters with unknown detection probability are provided in Section 3.2.

3.1 Augmented trajectory state space model

Refer to the method in the study of Wei et al. (2022), let $b \in \mathbb{B} = [0, 1]$ for the single trajectory detection probability space. It is worth noting that b represents the probability that the trajectory itself is detected by the sensor. The variable b is augmented into the single trajectory state to get the single augmented trajectory state with an auxiliary variable, such that $\bar{X} = (u, \hat{X}) \in \mathbb{U}_k \times \hat{\mathbb{X}}_k$, where $\mathbb{U}_k \times \hat{\mathbb{X}}_k$ represents the augmented trajectory state space with an auxiliary variable. $\hat{X} = \left(t, b^{1:\nu}, x^{1:\nu}\right) \in \hat{\mathbb{X}}_k$ denotes the single augmented trajectory state, and the augmented trajectory state space is given by

$$\hat{\mathbb{X}}_k = \uplus_{(t,\nu)\in I_k}\{t\} \times \mathbb{B}_k^{\nu} \times \mathbb{R}_k^{\nu n_x}. \tag{11}$$

$\hat{\mathbf{X}}_k \in \mathcal{F}\left(\bar{\mathbb{X}}_k\right)$ denotes the set of augmented trajectories.

To describe the TPMB filters with unknown detection probability, the alive trajectory state transition model, the all trajectories state transition model, and the trajectory measurement likelihood function based on the augmented trajectory state space model are redefined. In addition, $p^S\left(\bar{X}\right)$ represents trajectory survival probability as shown by García-Fernández et al. (2020c).

(1) Transition Model of the Augmented Trajectory State for the Set of Alive Trajectories

At time step k, the single alive trajectory $\hat{X} = \left(t, b^{1:\nu}, x^{1:\nu}\right) \in \hat{\mathbf{X}}_k$, where $t + \nu - 1 = k$ and $\hat{\mathbf{X}}_k$ is the set of alive trajectories , from time step k to $k+1$, either survives with probability $p^S(\hat{X}) = p^S(x^{\nu})$ with the transition density

$$\begin{aligned} g_{k+1}\left(t_y, b^{1:\nu_y}, x^{1:\nu_y}|\cdot\right) =& \delta_t\left[t_y\right]\delta_{\nu+1}\left[\nu_y\right]\delta_{x^{1:\nu}}\left[x^{1:\nu_y-1}\right] \\ &\times \delta_{b^{1:\nu}}\left[b^{1:\nu_y-1}\right] g_x\left(x^{\nu_y}|x^{\nu}\right) \\ &\times g_b\left(b^{\nu_y}|b^{\nu}\right), \end{aligned} \tag{12}$$

or dies with probability $1 - p^S(\hat{X})$.

(2) Transition Model of the Augmented Trajectory State for the Set of All Trajectories

At time step k, for the set of all trajectories $\hat{\mathbf{X}}_k$, the single trajectory $\hat{X} = \left(t, b^{1:\nu}, x^{1:\nu}\right) \in \hat{\mathbf{X}}_k$, where $t + \nu - 1 \le k$. The transition density from time step k to $k+1$ is as follows:

$$\begin{aligned} g_{k+1}\left(t_y, b^{1:\nu_y}, x^{1:\nu_y}|\cdot\right) =& \delta_t\left[t_y\right] \\ &\times \begin{cases} \delta_{\nu+1}[\nu_y]\delta_{x^{1:\nu}}[x^{1:\nu_y}]\delta_{b^{1:\nu}}[b^{1:\nu_y}], & \omega_y < k; \\ \delta_{\nu+1}[\nu_y]\delta_{x^{1:\nu}}[x^{1:\nu_y}] & \\ \times\delta_{b^{1:\nu}}[b^{1:\nu_y}](1 - p^S(\hat{X})), & \omega_y = k; \\ \delta_{\nu+1}[\nu_y]\delta_{x^{1:\nu}}[x^{1:\nu_y-1}]\delta_{b^{1:\nu}}[b^{1:\nu_y-1}] & \\ \times p^S(\hat{X}) g_x\left(x^{\nu_y}|x^{\nu}\right) g_b\left(b^{\nu_y}|b^{\nu}\right), & \omega_y = k+1, \end{cases} \end{aligned} \tag{13}$$

where, $\omega_y = t_y + \nu_y - 1$, $p^S(\hat{X}) = 1$.

(3) Birth Model of the Augmented Trajectory State

At time step k, the newborn augmented trajectories state are born independently following a PPP with intensity:

$$\lambda_k^{born}\left(t, b^{1:\nu}, x^{1:\nu}\right) = \delta_k\left[t\right]\delta_1\left[\nu\right]\lambda_b^{born}\left(b^{\nu}\right)\lambda_x^{born}\left(x^{\nu}\right). \tag{14}$$

Remark 1 The birth model of the augmented trajectory state of the set of all trajectories is the same as the set of alive trajectories.

(4) Measurement Model of the Augmented Trajectory State

The measurement model of the augmented trajectory state can be written for sets of all trajectories and sets of alive trajectories in the same manner.

At time step k, the single (alive or all) trajectory, $\hat{X} = \left(t, b^{1:\nu}, x^{1:\nu}\right) \in \hat{\mathbf{X}}_k$, is either detected with probability

$$p_{D,k}(\hat{X}) = \begin{cases} b^{\nu}\delta_{k-t+1}\left(\nu\right), & t+\nu-1=k; \\ 0, & otherwise, \end{cases} \tag{15}$$

and generates measurement with density

$$\begin{aligned} \phi\left(z_k|\hat{X}\right) &= \phi\left(z_k|t, b^{\nu}, x^{\nu}\right)\delta_{k-t+1}\left(\nu\right) \\ &= \phi_x\left(z_k|x^{\nu}\right)\delta_{k-t+1}\left(\nu\right), \end{aligned} \tag{16}$$

or undetected with probability $1 - p_{D,k}(\hat{X})$.

3.2 Recursion of TPMB filters with unknown detection probability

Given a real-valued function $\pi\left(\cdot\right)$ on the single augmented trajectory state space $\hat{\mathbb{X}}_k$, its integral is

$$\int \pi(\hat{X})d\hat{X} = \sum_{(t,\nu)\in I_k}\int\int \pi\left(t, b^{1:\nu}, x^{1:\nu}\right)db^{1:\nu}dx^{1:\nu}. \tag{17}$$

Since the probability of detection and the state of kinematic are independent, Eq.(17) can be rewritten as

$$\begin{aligned} \int \pi(\hat{X})d\hat{X} = \sum_{(t,\nu)\in I_k}&\int \pi_b\left(t, b^{1:\nu}\right)db^{1:\nu} \\ &\times \int \pi_x\left(t, x^{1:\nu}\right)dx^{1:\nu}. \end{aligned} \tag{18}$$

Given a real-valued function $\pi\left(\cdot\right)$ on the set of augmented trajectories space $\mathcal{F}\left(\hat{\mathbb{X}}_k\right)$, its integral is

$$\begin{aligned} &\int \pi(\hat{\mathbf{X}})\delta\hat{\mathbf{X}} \\ &\quad = \sum_{N_{\hat{\mathbf{X}}}=0}^{\infty}\frac{1}{N_{\hat{\mathbf{X}}}!}\int \pi\left(\left\{\hat{X}_1, \hat{X}_2, \ldots, \hat{X}_{N_{\hat{\mathbf{X}}}}\right\}\right)d\hat{X}_{1:N_{\hat{\mathbf{X}}}}, \end{aligned} \tag{19}$$

where $\int \pi(\hat{\mathbf{X}})\delta\hat{\mathbf{X}}$ is the set integral(Mahler, 2007, 2014), and $N_{\hat{\mathbf{X}}}$ is the number of elements in the set of trajectories $\hat{\mathbf{X}}$.

The inner product of two given functions real-valued $f\left(\cdot\right), g\left(\cdot\right)$ on the single augmented trajectory state space is computed as follows

$$\langle f, g\rangle = \int f(\hat{X})g(\hat{X})d\hat{X}. \tag{20}$$

Based on the above, the recursion of TPMB filter with unknown detection probability is proposed.

3.2.1 Prediction

Suppose that the parameters of TPMB density for the augmented trajectory state are λ_{k-1}^u and $\left\{r_{k-1}^i, p_{k-1}^i\right\}_{i=1}^{n_{k-1}}$ at time step k-1. At time step k, the predicted density is a TPMB density with $n_{k|k-1} = n_{k-1}$ and

$$\lambda_{k|k-1}(\hat{X}) = \lambda_k^{born}(\hat{X}) + \left\langle \lambda_{k-1}^u, g_k(\hat{X}|\cdot)p^S\left(\cdot\right)\right\rangle, \tag{21}$$

$$r_{k|k-1}^i = r_{k-1}^i\left\langle p_{k-1}^i, p^S\right\rangle, \tag{22}$$

$$p_{k|k-1}^i(\hat{X}) = \frac{\left\langle p_{k-1}^i, g_k(\hat{X}|\cdot)p^S\left(\cdot\right)\right\rangle}{\left\langle p_{k-1}^i, p^S\right\rangle}, \tag{23}$$

where λ_k^{born}, $g_k\left(\cdot|\cdot\right)$, $p^S\left(\cdot\right)$ are chosen depending on the case in Section 3.1 for alive trajectories and all trajectories.

3.2.2 Update

Suppose that the parameters of predicted TPMB density for the augmented trajectory state are $\lambda_{k|k-1}^u$ and $\left\{r_{k|k-1}^i, p_{k|k-1}^i\right\}_{i=1}^{n_{k|k-1}}$ at time step k and the measurement set $\mathbf{z}_k = \left\{z_k^1, z_k^2, \ldots, z_k^m\right\}$. Note that the TPMB density for the augmented trajectory state is updated to the TPMBM density. The parameters of TPMBM density are given as follows.

(1) Missed detection for PPP

$$\lambda_k^u(\hat{X}) = (1 - p_{D_k}(\hat{X}))\lambda_{k|k-1}(\hat{X}). \tag{24}$$

For each Bernoulli component i, $i \in \{1,2,\ldots,n_{k|k-1}\}$, there are $h^i = m_k + 1$ local hypotheses, and the set $\mathcal{M}(i,1+j) = j, j \in \{1,2,\ldots,m_k\}$ denotes the measurement z_k^j in the measurement set $\mathbf{z}_k$ corresponding to the local hypothesis j of the i-th Bernoulli component.

(2) Missed detection for Bernoulli component

$$w_k^{i,1} = 1 - r_{k|k-1}^i \left\langle p_{k|k-1}^i, p_{D_k}(\hat{X}) \right\rangle, \tag{25}$$

$$r_k^{i,1} = \frac{r_{k|k-1}^i \left\langle p_{k|k-1}^i, 1 - p_{D_k}(\hat{X}) \right\rangle}{1 - r_{k|k-1}^i \left\langle p_{k|k-1}^i, p_{D_k}(\hat{X}) \right\rangle}, \tag{26}$$

$$p_k^{i,1}(\hat{X}) = \frac{(1 - p_{D_k}(\hat{X}))p_{k|k-1}^i(\hat{X})}{\left\langle p_{k|k-1}^i, 1 - p_{D_k}(\hat{X}) \right\rangle}, \tag{27}$$

where the local hypothesis is given by $\mathcal{M}(i,1) = \emptyset$.

(3) Update for detected Bernoulli component

$$w_k^{i,1+j} = r_{k|k-1}^i \left\langle p_{k|k-1}^i, p_{D_k}(\hat{X}) \phi\left(z_k^j|\cdot\right) \right\rangle, \tag{28}$$

$$r_k^{i,1+j} = 1, \tag{29}$$

$$p_k^{i,1+j}(\hat{X}) = \frac{p_{k|k-1}^i p_{D_k}(\hat{X}) \phi\left(z_k^j|\cdot\right)}{\left\langle p_{k|k-1}^i, p_{D_k}(\hat{X}) \phi\left(z_k^j|\cdot\right) \right\rangle}, \tag{30}$$

where the local hypothesis is given by $\mathcal{M}(i,1+j) = \{j\}$.

(4) New Bernoulli component for the first time

According to García-Fernández et al. (2020c), each measurement generates a new Bernoulli component, let be the new Bernoulli component $i = n_{k|k-1} + j$, $j \in \{1,2,\ldots,m_k\}$, which is caused by measurement z_k^j. The number of local hypotheses for i-th Bernoulli component is $h_i = 2$, $\mathcal{M}(i,1) = \emptyset$, $w_k^{i,1} = 1$, $r_k^{i,h_i} = 0, \mathcal{M}(i,2) = \{j\}$,

$$w_k^{i,2} = \lambda^C\left(z_k^j\right) + \left\langle \lambda_{k|k-1}, p_{D_k}(\hat{X}) \phi\left(z_k^j|\cdot\right) \right\rangle, \tag{31}$$

$$r_k^{i,2} = \frac{\left\langle \lambda_{k|k-1}^i, p_{D_k}(\hat{X}) \phi\left(z_k^j|\cdot\right) \right\rangle}{\lambda^C\left(z_k^j\right) + \left\langle \lambda_{k|k-1}^i, p_{D_k}(\hat{X}) \phi\left(z_k^j|\cdot\right) \right\rangle}, \tag{32}$$

$$p_k^{i,2}(\hat{X}) = \frac{\lambda_{k|k-1}^i p_{D_k}(\hat{X}) \phi\left(z_k^j|\cdot\right)}{\left\langle \lambda_{k|k-1}^i, p_{D_k}(\hat{X}) \phi\left(z_k^j|\cdot\right) \right\rangle}. \tag{33}$$

The set of global hypotheses is as follows(García-Fernández et al., 2020c):

$$\mathcal{A}_k = \left\{ (a_1, a_2, \ldots, a_{n_k}) : a_i \in \mathbb{N}_{h^i}, \bigcup_{i=1}^{n_k} \mathcal{M}(i, a_i) = \mathbb{N}_{m_k}, \right.$$
$$\left. \mathcal{M}(i, a_i) \bigcap \mathcal{M}(j, a_j) = 0 \forall i \neq j \right\}, \tag{34}$$

where $\mathbb{N}_{m_k} = (1,2,\ldots,m_k)$, $n_k = n_{k|k-1} + m_k$.

After the above Bernoulli updates, the TPMB density is updated to the TPMBM density. To ensure the closed form of the recursion, the TPMBM density should be approximated to the TPMB density(García-Fernández et al., 2020c).

4 BG TPMB filters

This section introduces the BG implementation of the TPMB filters with unknown detection probability. It provides prediction and update for both alive and all trajectories. BG implementation for the alive trajectories is given in Section 4.1, and BG implementation for all trajectories is given in Section 4.2.

The beta distribution of a single trajectory detection probability is as follows:

$$\mathcal{B}\left(t, b^{1:\nu}; \tau, \bar{u}, \bar{v}\right) = \begin{cases} \mathcal{B}\left(b^{1:\nu}; \tau, \bar{u}, \bar{v}\right), & t = \tau, \nu = l; \\ 0, & otherwise, \end{cases} \tag{35}$$

where $\bar{u}, \bar{v} \in \mathbb{R}^l$, l is the length of the trajectory, and t is the initial time of the trajectory. The beta distribution is as follows:

$$\begin{aligned} \mathcal{B}(b; u, v) &= \frac{b^{u-1}(1-b)^{v-1}}{\int_0^1 b^{u-1}(1-b)^{v-1} db} \\ &= \frac{b^{u-1}(1-b)^{v-1}}{\mathcal{B}(b; u, v)}, \end{aligned} \tag{36}$$

where, $0 \leq b \leq 1$, $u > 1$, $v > 1$. The expectation of $\mathcal{B}(\eta; s, t)$ is $\mu = u/(u+v)$. The covariance of $\mathcal{B}(\eta; s, t)$ is $\sigma^2 = uv/\left((u+v)^2(u+v+1)\right)$.

The Gaussian distribution of the kinematic state for a single trajectory is as follows:

$$\mathcal{N}\left(t, x^{1:\nu}; \tau, \bar{x}, P\right) = \begin{cases} \mathcal{N}\left(x^{1:\nu}; \tau, \bar{x}, P\right), & t = \tau, \nu = l; \\ 0, & otherwise, \end{cases} \tag{37}$$

where $\bar{x} \in \mathbb{R}^{ln_x}$ is mean and $P \in \mathbb{R}^{ln_x \times ln_x}$ is covariance matrix.

Thus, the trajectory BG function is given as follows:

$$BG\left(\hat{X};\tau,\varsigma\right)=\mathcal{B}\left(b^{1:\nu};\tau,\bar{u},\bar{v}\right)\mathcal{N}\left(x^{1:\nu};\tau,\bar{x},P\right), \tag{38}$$

where, $\varsigma=(\bar{u},\bar{v},\bar{x},P)$.

In addition, the following assumptions are needed:

(1) The survival probability of a single trajectory is $p^S\left(x^\nu\right)=p^S$.

(2) $g_x\left(\cdot|x^\nu\right)=\mathcal{N}\left(\cdot;Fx^\nu,P\right)$, $\phi_x\left(\cdot|x^\nu\right)=\mathcal{N}\left(\cdot;Hx^\nu,R\right)$.

(3) The Poisson intensity of birth at time step k is as follows:

$$\lambda_k^{born}(\hat{X})=\sum_{q=1}^{n_k^{born}}w_k^{born,q}BG\left(\hat{X};k,\bar{u}_k^{born,q},\bar{v}_k^{born,q},\bar{x}_k^{born,q},P_k^{born,q}\right), \tag{39}$$

where n_k^{born} is the number of components at time step k, $w_k^{born,q}$ is weight of the q-th component, $t^{born,q}=k$ is the start time, $\bar{u}_k^{born,q},\bar{v}_k^{born,q}$ are the beta distribution parameters, $\bar{x}_k^{born,q}$ is the mean of a Gaussian distribution and $P_k^{born,q}$ is the covariance matrix of a Gaussian distribution.

(4) The Poisson intensity at time step $k-1$ is as follows:

$$\lambda_{k-1}(\hat{X})=\sum_{q=1}^{n_{k-1}^p}w_{k-1}^{p,q}BG\left(\hat{X};t_{k-1}^{p,q},\bar{u}_{k-1}^{p,q},\bar{v}_{k-1}^{p,q},\bar{x}_{k-1}^{p,q},P_{k-1}^{p,q}\right), \tag{40}$$

where n_{k-1}^p is the number of components, $w_{k-1}^{p,q}$ is weight of the q-th component, $t_{k-1}^{p,q}$ is the start time, $\bar{u}_{k-1}^{p,q},\bar{v}_{k-1}^{p,q}$ are the beta distribution parameters, $\bar{x}_{k-1}^{p,q}$ is the mean of Gaussian distribution, and $P_{k-1}^{p,q}$ is the covariance matrix of Gaussian distribution.

4.1 BG implementation for alive trajectories

In the implementation of BG for alive trajectories, the density of the single alive trajectory of the i-th Bernoulli component at time step k-1 is considered as follows:

$$p_{k-1}^i(\hat{X})=BG\left(\hat{X};t^i,\bar{u}_{k-1}^i,\bar{v}_{k-1}^i,\bar{x}_{k-1}^i,P_{k-1}^i\right), \tag{41}$$

where t^i is the start time, $\bar{u}_{k-1}^i,\bar{v}_{k-1}^i$ are the beta distribution parameters, $\bar{x}_{k-1}^i$ is the mean of Gaussian, and P_{k-1}^i is the covariance matrix of Gaussian. $dim\left(\bar{u}_{k-1}^i\right)=dim\left(\bar{v}_{k-1}^i\right)=dim\left(\bar{x}_{k-1}^i\right)/n_x$ is the length of trajectory, where $dim\left(\cdot\right)$ denotes the variable dimension. $t^i+dim\left(\bar{x}_{k-1}^i\right)/n_x-1=k$ implies that the trajectory is alive at time step k.

The prediction step and update step for alive trajectories are given by the following propositions.

Proposition 1 Suppose that at time $k-1$, the updated parameters of the TPMB are $\left\{\lambda_{k-1},\left\{r_{k-1}^i,p_{k-1}^i\right\}_{i=1}^{n_{k-1}}\right\}$, where λ_{k-1} and p_{k-1}^i are given in Eqs (40) and (41). The prediction step of BG implementation for alive trajectories is divided into two parts, PPP and MB, as follows.

(1) PPP

$$\lambda_{k|k-1}(\hat{X})=p^S\sum_{q=1}^{n_{k-1}^p}w_{k-1}^{p,q}BG\left(\hat{X};t_{k-1}^{p,q},\bar{u}_{k|k-1}^{p,q},\bar{v}_{k|k-1}^{p,q},\bar{x}_{k|k-1}^{p,q},P_{k|k-1}^{p,q}\right)+\lambda_k^{born}(\hat{X}), \tag{42}$$

where $\lambda_k^{born}(\hat{X})$ is given by form (39), and

$$\bar{u}_{k|k-1}^{p,q}=\left[\left(\bar{u}_{k-1}^{p,q}\right),u_{k|k-1}^{p,q}\right]^{\mathrm{T}}, \tag{43a}$$

$$\bar{v}_{k|k-1}^{p,q}=\left[\left(\bar{v}_{k-1}^{p,q}\right),v_{k|k-1}^{p,q}\right]^{\mathrm{T}}, \tag{43b}$$

$$\bar{x}_{k|k-1}^{p,q}=\left[\left(\bar{x}_{k-1}^{p,q}\right),\left(\bar{F}_i\bar{x}_{k|k-1}^{p,q}\right)^{\mathrm{T}}\right]^{\mathrm{T}}, \tag{43c}$$

$$P_{k|k-1}^{p,q}=\begin{bmatrix}P_{k-1}^{p,q}, & P_{k-1}^{p,q}\bar{F}_i^{\mathrm{T}}\\ \bar{F}_iP_{k-1}^{p,q}, & \bar{F}_iP_{k-1}^{p,q}\bar{F}_i^{\mathrm{T}}+Q\end{bmatrix}, \tag{43d}$$

$$\bar{F}_i=[0_{1,l^{p,q}-1},1]\otimes F, \tag{43e}$$

$$v_{k|k-1}^{p,q}=\left(\frac{\mu\left(1-\mu\right)}{\left(\sigma\right)^2}-1\right)\left(1-\mu\right), \tag{43f}$$

$$u_{k|k-1}^{p,q}=\left(\frac{\mu\left(1-\mu\right)}{\left(\sigma\right)^2}-1\right)\mu, \tag{43g}$$

$$\mu=\frac{u}{u+v}, \tag{43h}$$

$$\left(\sigma\right)^2=\rho\frac{uv}{\left(u+v\right)^2\left(u+v+1\right)}, \tag{43i}$$

$$u=[0_{1,l^{p,q}-1},1]\,\bar{u}_{k-1}^{p,q}, \tag{43j}$$

$$v=[0_{1,l^{p,q}-1},1]\,\bar{v}_{k-1}^{p,q}, \tag{43k}$$

where $\otimes$ is Kronecker product, $l^{p,q}=dim\left(\bar{x}_{k-1}^{p,q}\right)/n_x$,$0_{m,n}$ is the $m\times n$ zeros matrix, and $\rho>1$ is a constant.

(2) MB

$$r_{k|k-1}^{i} = p^{S} r_{k-1}^{i}, \tag{44a}$$

$$p_{k|k-1}^{i} = BG\left(\hat{X}; t^{i}, \bar{u}_{k|k-1}^{i}, \bar{v}_{k|k-1}^{i}, \bar{x}_{k|k-1}^{i}, P_{k|k-1}^{i}\right), \tag{44b}$$

where $\bar{u}_{k|k-1}^{i}, \bar{v}_{k|k-1}^{i}, \bar{x}_{k|k-1}^{i}, P_{k|k-1}^{i}$ are calculated by replacing $\bar{u}_{k-1}^{p,q}$, $\bar{v}_{k-1}^{p,q}$, $\bar{x}_{k-1}^{p,q}$, $P_{k-1}^{p,q}$ of Eq.(43) with $\bar{u}_{k-1}^{i}, \bar{v}_{k-1}^{i}, \bar{x}_{k-1}^{i}, P_{k-1}^{i}$.

Proof: The proof of Proposition 1 is provided in the Supplementary Materials.

Proposition 2 Suppose that at time k, the predicted parameters of the TPMB are $\left\{\lambda_{k|k-1}, \left\{r_{k|k-1}^{i}, p_{k|k-1}^{i}\right\}_{i=1}^{n_{k|k-1}}\right\}$, where $r_{k|k-1}^{i}$ and $p_{k|k-1}^{i}$ are given in Eq.(44a,b), $n_{k|k-1} = n_{k-1}$, $\lambda_{k|k-1}$ is given by Eq.(42), and $\lambda_{k|k-1}$ is rewritten as

$$\lambda_{k|k-1}(\hat{X}) = \sum_{q=1}^{n_{k|k-1}^{p}} w_{k|k-1}^{p,q} BG\left(\hat{X}; t_{k-1}^{p,q}, \bar{u}_{k|k-1}^{p,q}, \bar{v}_{k|k-1}^{p,q}, \bar{x}_{k|k-1}^{p,q}, P_{k|k-1}^{p,q}\right), \tag{45}$$

where $n_{k|k-1}^{p} = n_{k-1}^{p} + n_{k}^{born}$.

The update density can be considered from four cases, which are given as follows.

(1) Missed detection for PPP

$$\lambda_{k}(\hat{X}) = \sum_{q=1}^{n_{k}^{p}} w_{k}^{p,q} BG\left(\hat{X}; t_{k}^{p,q}, \bar{u}_{k}^{p,q}, \bar{v}_{k}^{p,q}, \bar{x}_{k}^{p,q}, P_{k}^{p,q}\right), \tag{46}$$

where

$$w_{k}^{p,q} = w_{k|k-1}^{p,q} \frac{v^{p,q}}{u^{p,q} + v^{p,q}}, \tag{47a}$$

$$t_{k}^{p,q} = t_{k-1}^{p,q}, \tag{47b}$$

$$\bar{u}_{k}^{p,q} = \bar{u}_{k|k-1}^{p,q}, \tag{47c}$$

$$\bar{v}_{k}^{p,q} = \left[1_{1,l^{p,q}-1}, 0\right]^{T} \odot \bar{v}_{k|k-1}^{p,q} + \left[0_{1,l^{p,q}-1}, 1\right]^{T} \left(v^{p,q} + 1\right), \tag{47d}$$

$$\bar{x}_{k}^{p,q} = \bar{x}_{k|k-1}^{p,q}, \tag{47e}$$

$$P_{k}^{p,q} = P_{k|k-1}^{p,q}, \tag{47f}$$

where $l^{p,q} = dim\left(\bar{u}_{k|k-1}^{p,q}\right)$, $u^{p,q}$, $v^{p,q}$ are obtained by Eqs (43j) and (43k) using $\bar{u}_{k|k-1}^{p,q}$ and $\bar{v}_{k|k-1}^{p,q}$ instead of $\bar{u}_{k-1}^{p,q}$ and $\bar{v}_{k-1}^{p,q}$, and $A \odot B$ represents matrix dot product, that is, the multiplication of the corresponding elements of the matrix A and B.

(2) Missed detection for Bernoulli component

$$w_{k}^{i,1} = 1 - r_{k|k-1}^{i} \frac{u^{i}}{u^{i} + v^{i}}, \tag{48a}$$

$$r_{k}^{i,1} = \frac{r_{k|k-1}^{i} \frac{v^{i}}{u^{i}+v^{i}}}{1 - r_{k|k-1}^{i} \frac{u^{i}}{u^{i}+v^{i}}}, \tag{48b}$$

$$p_{k}^{i,1}(\hat{X}) = BG\left(\hat{X}; t^{i}, \bar{u}_{k}^{i,1}, \bar{v}_{k}^{i,1}, \bar{x}_{k}^{i,1}, P_{k}^{i,1}\right), \tag{48c}$$

where

$$\bar{u}_{k}^{i,1} = \bar{u}_{k|k-1}^{i}, \tag{49a}$$

$$\bar{v}_{k}^{i,1} = \left[1_{1,l^{i}-1}, 0\right]^{T} \odot \bar{v}_{k|k-1}^{i} + \left[0_{1,l^{i}-1}, 1\right]^{T} \left(v^{i} + 1\right), \tag{49b}$$

$$\bar{x}_{k}^{i,1} = \bar{x}_{k|k-1}^{i}, \tag{49c}$$

$$P_{k}^{i,1} = P_{k|k-1}^{i}, \tag{49d}$$

where $l^{i} = dim\left(\bar{u}_{k|k-1}^{i}\right)$, u^{i}, v^{i} are obtained by Eqs (43j) and (43k) using $\bar{u}_{k|k-1}^{i}$ and $\bar{v}_{k|k-1}^{i}$ instead of $\bar{u}_{k-1}^{p,q}$ and $\bar{v}_{k-1}^{p,q}$.

(3) Update for detected Bernoulli component

For the Bernoulli component i and measurement z_{k}^{j},

$$w_{k}^{i,1+j} = r_{k|k-1}^{i} \frac{u^{i}}{u^{i} + v^{i}} \mathcal{N}\left(z_{k}^{j}; \bar{z}_{i}, S_{i}\right), \tag{50a}$$

$$p_{k}^{i,1+j}(\hat{X}) = BG\left(\hat{X}; t^{i}, \bar{u}_{k}^{i,1+j}, \bar{v}_{k}^{i,1+j}, \bar{x}_{k}^{i,1+j}, P_{k}^{i,1+j}\right), \tag{50b}$$

$$\bar{u}_{k}^{i,1+j} = \left[1_{1,l^{i}-1}, 0\right]^{T} \odot \bar{u}_{k|k-1}^{i} + \left[0_{1,l^{i}-1}, 1\right]^{T} \left(u^{i} + 1\right), \tag{50c}$$

$$\bar{v}_{k}^{i,1+j} = \bar{v}_{k|k-1}^{i}, \tag{50d}$$

$$\bar{z}_{i} = \bar{H}_{i} \bar{x}_{k}^{i}, \tag{50e}$$

$$S_{i} = \bar{H}_{i} P_{k|k-1}^{i} \bar{H}_{i}^{T} + R, \tag{50f}$$

$$\bar{H}_{i} = \left[0_{1,l^{i}-1}, 1\right] \otimes H, \tag{50g}$$

$$\bar{x}_{k}^{i,1+j} = \bar{x}_{k|k-1}^{i} + P_{k|k-1}^{i} \bar{H}_{i}^{T} S_{i}^{-1} \left(z_{k}^{j} - \bar{z}_{i}\right), \tag{50h}$$

$$P_{k}^{i,1+j} = P_{k|k-1}^{i} - P_{k|k-1}^{i} \bar{H}_{i}^{T} S_{i}^{-1} \bar{H}_{i} P_{k|k-1}^{i}. \tag{50i}$$

(4) New Bernoulli component for the first time

For the new Bernoulli component $i = n_{k|k-1}+j$ generated by measurement $z_k^j, j \in \{1,2,\ldots,m_k\}$. For the new Bernoulli component, as seen above, it is updated from the predicted Poisson density and corresponds to a new trajectory. The BG component with the greatest weight is selected, and the parameters of the new Bernoulli component are determined by $w_k^{i,1}=1$, $r_k^{i,1}=0$,

$$w_k^{i,2} = \lambda^C\left(z_k^j\right) + \sum_{q=1}^{n_{k|k-1}^p} s^q, \tag{51a}$$

$$r_k^{i,2} = \frac{\sum_{q=1}^{n_{k|k-1}^p} s^q}{w_k^{i,2}}, \tag{51b}$$

$$p_k^{i,2}\left(\hat{X}\right) = BG\left(\hat{X}; t_{k|k-1}^{p,q*}, \bar{u}_k^{i,2}, \bar{v}_k^{i,2}, \bar{x}_k^{i,2}, P_k^{i,2}\right), \tag{51c}$$

where

$$\bar{u}_k^{i,2} = \left[1_{1,l^i-1},0\right]^T \odot \bar{u}_{k|k-1}^{p,q*} + \left[0_{1,l^i-1},1\right]^T\left(u^{q*}+1\right), \tag{52a}$$

$$\bar{v}_k^{i,2} = \bar{v}_{k|k-1}^{p,q^*}, \tag{52b}$$

$$\bar{x}_k^{i,2} = \bar{x}_{k|k-1}^{p,q^*} + P_{k|k-1}^{p,q^*}\bar{H}_i^T S_{q^*}^{-1}\left(z_k^j - \bar{z_{q^*}}\right), \tag{52c}$$

$$P_k^{i,2} = P_{k|k-1}^{p,q^*} - P_{k|k-1}^{p,q*}\bar{H}_{q^*}^T S_{q^*}^{-1}\bar{H}_{q^*}P_{k|k-1}^{p,q^*}, \tag{52d}$$

$$\bar{z_{q^*}} = \bar{H}_{q^*}\bar{x}_{k|k-1}^{p,q^*}, \tag{52e}$$

where $q^* = \max_q\left(s^q\right), q \in \left\{1,2,\ldots,n_{k|k-1}^p\right\}$ and s^q is given by

$$s^q = \frac{u^q}{u^q+v^q}\mathcal{N}\left(z_k^j; \bar{z_q}, S_q\right), \tag{53a}$$

$$\bar{z_q} = \bar{H}_q\bar{x}_{k|k-1}^{p,q}, \tag{53b}$$

$$\bar{H}_q = [0_{1,l^{p,q}-1},1]\otimes H, \tag{53c}$$

$$S_q = \bar{H}_q P_{k|k-1}^{p,q}\bar{H}_q^T + R, \tag{53d}$$

where $l^{p,q} = dim\left(\bar{u}_{k|k-1}^{p,q}\right)$, u^q, v^q are obtained by Eqs (43j) and (43k) using $\bar{u}_{k|k-1}^{p,q}$ and $\bar{v}_{k|k-1}^{p,q}$ instead of $\bar{u}_{k-1}^{p,q}$ and $\bar{v}_{k-1}^{p,q}$.

Proof:The proof of Proposition 2 is provided in the Supplementary Materials.

Remark 2 After the above updating process, the predicted PMB density is updated to the PMBM density. Then, the PMBM density is approximated to a PMB filter. To obtain the single trajectory density, $p(\cdot)$ is a BG mixture, adopting KLD minimization to fit the BG distribution. Before Bernoulli merges, the distance between two BG distributions needs to be calculated. However, the purpose of target tracking is to detect and track, not to calculate the detailed detection probability. Therefore, it is necessary to determine the distance between the two Gaussian distributions. The BG mixture is then merged using criteria similar to the merging criteria for Gaussian mixtures(Mahler, 2007; García-Fernández et al., 2020c; Bishop, 2006).

The results are given in the Supplementary Materials.

4.2 BG implementation for all trajectories

In the BG implementation for all trajectories, focus on all trajectories that have been detected. Suppose the single trajectory density of the i-th Bernoulli component at time step k-1 is as follows:

$$p_{k-1}^i(\hat{X}) = \sum_{\varphi=t^i}^{k-1}\beta_{k-1}^i(\varphi)\,BG(\hat{X}; t^i, \bar{u}_{k-1}^i(\varphi), \bar{v}_{k-1}^i(\varphi), \bar{x}_{k-1}^i(\varphi), P_{k-1}^i(\varphi)), \tag{54}$$

where t^i is the start time of the single trajectory, $\beta_{k-1}^i(\varphi)$ denotes the termination probability that the corresponding single trajectory at time step φ(García-Fernández et al., 2020c), $\bar{u}_{k-1}^i(\varphi) \in \mathbb{R}^l$, $\bar{v}_{k-1}^i(\varphi) \in \mathbb{R}^l$, $\bar{x}_{k-1}^i(\varphi) \in \mathbb{R}^{ln_x}$, $P_{k-1}^i(\varphi) \in \mathbb{R}^{ln_x \times ln_x}$, $l = \varphi - t^i + 1$, and $\sum_{\varphi=t^i}^{k-1}\beta_{k-1}^i(\varphi) = 1$.

The prediction step and update step for all trajectories are given by the following propositions.

Proposition 3 Suppose that at time $k-1$, the updated parameters of the TPMB are $\left\{\lambda_{k-1}, \left\{r_{k-1}^i, p_{k-1}^i\right\}_{i=1}^{n_{k-1}}\right\}$, where λ_{k-1} and p_{k-1}^i are given in Eqs (40) and (54). $\lambda_{k|k-1}$ is given by Eq.(42) and $r_{k|k-1}^i = r_{k-1}^i$. The BG parameters of Eq.(54), for $\varphi \in \left\{t^i,\ldots,k-1\right\}$, are $\bar{u}_{k|k-1}^i(\varphi) = \bar{u}_{k-1}^i(\varphi)$, $\bar{v}_{k|k-1}^i(\varphi) = \bar{v}_{k-1}^i(\varphi)$, $\bar{x}_{k|k-1}^i(\varphi) = \bar{x}_{k-1}^i(\varphi)$, $P_{k|k-1}^i(\varphi) = P_{k-1}^i(\varphi)$, and for $\varphi = k$, $\bar{u}_{k|k-1}^i(\varphi), \bar{v}_{k|k-1}^i(\varphi), \bar{x}_{k|k-1}^i(\varphi), P_{k|k-1}^i(\varphi)$ are given by Proposition 1. Then $\beta_{k|k-1}^i(\varphi)$ is given by

$$\beta_{k|k-1}^i(\varphi) = \begin{cases} \beta_{k-1}^i(\varphi), & \varphi \in \left\{t^i, t^i+1, \ldots, k-2\right\}; \\ \left(1-P^S\right)\beta_{k-1}^i(\varphi), & \varphi = k-1; \\ P^S\beta_{k-1}^i(k-1), & \varphi = k. \end{cases} \tag{55}$$

The proof of Proposition 3 is similar to the proof of Proposition 1. The detailed proof of Proposition

1 is provided, so the detailed proof of Proposition 3 will not be given.

Remark 3 Refer to García-Fernández et al. (2020c) ,the single trajectory density that considers the trajectory dead $\varphi \leq k-2$ is not modified. For the trajectory may terminate, $\varphi = k-1$, only change in the $\beta^i_{k|k-1}(\varphi)$ as one has to take into account the probability $\left(1-P^S\right)$. For the alive trajectory, $\varphi = k$, the parameters of BG are propagated as in the case of alive trajectories, see Proposition 1, and $\beta^i_{k|k-1}(\varphi)$ is $P^S\beta^i_{k-1}(k-1)$.

Proposition 4 Suppose the predicted density of TPMB as stated earlier, $p^i_{k|k-1}$ and $\lambda_{k|k-1}$ are given in Eqs (54) and (45). The missed detection of PPP intensity λ_k is given by Eq.(46). The misdetection hypothesis of i-th Bernoulli component has the following parameters:

$$w^{i,1}_k = 1 - r^i_{k|k-1}\beta^i_{k|k-1}(k)\, p^D_i, \tag{56a}$$

$$r^{i,1}_k = \frac{r^i_{k|k-1}\beta^i_{k|k-1}(k)\, p^D_i}{1 - r^i_{k|k-1}\beta^i_{k|k-1}(k)\, p^D_i}, \tag{56b}$$

$$\beta^{i,1}_k(\varphi) = \begin{cases} \beta^i_{k-1}(\varphi), & \varphi \in \left\{t^i, \ldots, k-1\right\}; \\ p^D_i\beta^i_{k-1}(\varphi), & \varphi = k, \end{cases} \tag{56c}$$

$$p^D_i = \frac{u^i(k)}{u^i(k) + v^i(k)}, \tag{56d}$$

$$u^i(k) = \left[0_{1,l^i-1}, 1\right]\bar{u}^i_{k-1}(k), \tag{56e}$$

$$v^i(k) = \left[0_{1,l^i-1}, 1\right]\bar{v}^i_{k-1}(k), \tag{56f}$$

where $l^i = dim\left(\bar{u}^i_{k-1}(k)\right)$.

The BG parameters of the trajectory density are as follows

$$\bar{u}^{i,1}_k(\varphi) = \bar{u}^i_{k|k-1}(\varphi), \tag{57a}$$

$$\bar{x}^{i,1}_k(\varphi) = \bar{x}^i_{k|k-1}(\varphi), \tag{57b}$$

$$P^{i,1}_k(\varphi) = P^i_{k|k-1}(\varphi), \tag{57c}$$

$$\bar{u}^{i,1}_k(\varphi) = \begin{cases} \bar{u}^{i,1}_{k|k-1}(\varphi), & \varphi \in \left\{t^i, \ldots, k-1\right\}; \\ \bar{u}^{i,1}_k(\varphi), & \varphi = k, \end{cases} \tag{57d}$$

where $\varphi \in \left\{t^i, \ldots, k\right\}$, $\bar{u}^{i,1}_k(k)$ is given by substituting $\bar{u}^i_{k|k-1}(k)$ into Eq.(49b).

For the Bernoulli component i and measurement z^j_k,

$$w^{i,1+j}_k = r^i_{k|k-1}\beta^i_{k|k-1}(k)\, p^D_i \mathcal{N}\left(z^j_k; \bar{z}_i, S_i\right), \tag{58a}$$

$$r^{i,1+j}_k = 1, \tag{58b}$$

$$\beta^{i,1+j}_k(\varphi) = \begin{cases} 0, & \varphi \in \left\{t^i, \ldots, k-1\right\}; \\ 1, & \varphi = k, \end{cases} \tag{58c}$$

$$p^{i,1+j}_k\left(\hat{X}\right) = BG\left(\hat{X}; t^i, \bar{u}^{i,1+j}_k, \bar{v}^{i,1+j}_k, \bar{x}^{i,1+j}_k, P^{i,1+j}_k\right), \tag{58d}$$

$$\tag{58e}$$

where $\bar{z}_i$, S_i, $\bar{u}^{i,1+j}_k$, $\bar{v}^{i,1+j}_k$, $\bar{x}^{i,1+j}_k$, $P^{i,1+j}_k$ are given by substituting $\bar{u}^i_{k|k-1}(k)$, $\bar{v}^i_{k|k-1}(k)$, $\bar{x}^i_{k|k-1}(k)$, $P^i_{k|k-1}(k)$ into Eqs (50c)-(50d) and Eqs (50h)-(50i), p^D_i is given by Eq.(56d).

The new Bernoulli component $i \in \left\{n_{k|k-1}+j\right\}$ is the same as the new Bernoulli component in the TPMB of the alive trajectories above, but only the Poisson intensity of the alive trajectories is considered in this section. Then $\beta^{i,2}_k(\varphi)$ of new Bernoulli component i is set to $\beta^{i,2}_k(k) = 1$ and $\beta^{i,2}_k(\varphi) = 0, \forall \varphi \neq k$.

The Bernoulli merge of all trajectories is the same as the Bernoulli merge of the alive trajectories, in addition,

$$\beta^i_k(\varphi) = \sum_{a^i=1:r^{i,a^i}_k>0}^{h_i}\left[\frac{\bar{w}^{i,a^i}_k r^{i,a^i}_k}{r^{i,}_k}\beta^{i,a^i}_k(\varphi)\right], \quad l \in \left\{t^i, \ldots, k\right\}. \tag{59}$$

For $\varphi = k$, the proof of Proposition 4 is the same as Proposition 2, and for $\varphi \neq k$, the trajectory state is not updated. Therefore the proof of Proposition 4 is omitted from this paper.

4.3 Estimation

According to García-Fernández et al. (2020c), the trajectory estimation of the updated posterior of Proposition 2 for alive trajectories at the time step k is $\left\{\left(t^i, \bar{b}^i, \bar{x}^i\right) : r^i_k > \Gamma_d\right\}$, which denotes the starting times, the mean of beta, and the mean of Gaussian of Bernoulli components whose r^i_k is satisfied with $r^i_k > \Gamma_d$. The mean of beta is estimated as follows

$$\bar{b}^i_k = \frac{\bar{u}^i_k}{\bar{u}^i_k + \bar{v}^i_k}. \tag{60}$$

For the trajectory estimation of the updated posterior of Proposition 4 for all trajectories at the time step k is $\left\{\left(t^i, \bar{b}^i(l^*), \bar{x}^i(l^*)\right) : r^i_k > \Gamma_d, l^* = \arg\max_l \beta^i_k(l)\right\}$, which denotes the starting times, the mean of beta, and the mean of Gaussian of Bernoulli components

whose probability of existence is greater than Γ_d. $\bar{b}^i(l^*)$ is obtained substituting $\bar{u}^i(l^*)$ and $\bar{v}^i(l^*)$ into Eq.(61). This paper assumes that all locus source observations are generated at the same time according to the same detection probability. Then, the final output of the detection probability estimate can be averaged by all the selected Bernoulli components. Thus, the detection probability is estimated as follows:

$$\hat{b}_k = \frac{1}{\bar{N}_k} \sum_{i=1}^{\bar{N}_k} \bar{b}_k^i, \tag{61}$$

where $\bar{N}$ is the number of estimated trajectories, that is, the number of Bernoulli components whose probability of existence is greater than Γ_d.

Finally, since TPMB filters with unknown detection probabilities have the same filter recursion for live trajectories and all trajectories, an algorithm is used to display the pseudocode for TPMB filters with unknown detection probability.

Algorithm 1 Beta-Gaussian TPMB Filters Pseudocodes.

Input: λ_{k-1}^u, r_{k-1}^i, p_{k-1}^i, n_{k-1}, $\mathbf{z}_k$

Prediction:

- For alive trajectories: use Proposition 1.
- For all trajectories: use Proposition 3.

Update:

- For alive trajectories: use Proposition 2.
- For all trajectories: use Proposition 4.

Merge the Bernoulli components:

for: $i = 1$ to n_k **do**

- r_k^{i,a^i} and $\bar{w}_k^{i,a^i}$ are calculated by Eqs (8) and (10).
- For alive trajectories: $\bar{u}_k^i$, $\bar{v}_k^i$, $\bar{x}_k^i$ and P^i are calculated by Eqs (75)-(82).
- For all trajectories: $\beta_k^i(k)$, $\bar{u}_k^i(k)$, $\bar{v}_k^i(k)$, $\bar{x}_k^i(k)$ and $P_k^i(k)$ are calculated by Eqs (83)-(91).

end for

Output: λ_k^u, r_k^i, p_k^i, n_k

5 Simulation results

This section analyzes the performance of the proposed two BG-TPMB filters based on the scenario used by García-Fernández et al. (2020c) and compares them with Beta Gaussian-TPHD (BG-TPHD)(Wei et al., 2022) and the standard TPMB. In standard TPMB, the detection probability is known and given as a prior. Consider four targets in the scenario, and the true trajectory is shown in Figure 1. The target kinematic state is denoted as $x = [p_x, \dot{p_x}, p_y, \dot{p_y}]$, where $[p_x, p_y]^T$ is 2-D position vector and $[\dot{p_x}, \dot{p_y}]$ is the corresponding velocity vector.

Consider the detection probability state $b = [u, v]$. All targets in the scenario follow a nearly constant velocity model, with the kinematic state transition matrix and process noise covariance given as follows:

$$F = I_2 \otimes \begin{bmatrix} 1, & T \\ 0, & 1 \end{bmatrix}, Q = qI_2 \otimes \begin{bmatrix} T^3/3, & T^2/2 \\ T^2/2, & T \end{bmatrix},$$

where I_2 is the identity matrix of order 2, $T = 1$ is sampling interval and $q = 0.01$. The trajectory survival probability is set to $p^S = 0.99$. The measurement generator matrix and measurement noise covariance are as follows:

$$H = \begin{bmatrix} 1, & 0, & 0, & 0 \\ 0, & 0, & 1, & 0 \end{bmatrix}, R = \sigma_R^2 I_2,$$

where $\sigma_R^2 = 1$. The number of clutter is distributed according to the Poisson distribution with a mean value of $\bar{\lambda}_C = 10$ and the clutter density is the uniform density in $[0, 300] \times [0, 300]$.

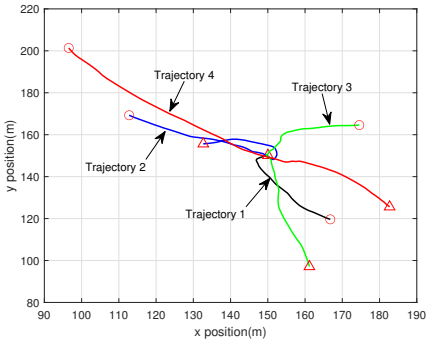

Fig. 1 True trajectories: four truth trajectories are shown in four different colors. The circle indicates the starting position of the trajectory, and the triangle indicates the vanishing position of the trajectory.

The Poisson birth intensity of trajectories is BG mixture with $x_k^{b,1} = [100, 0, 100, 0]^T$, $P_k^{b,1} = \mathrm{diag}([100, 1, 100, 1])$, with weight $w_k^{b,1} = 1$, $k = 1$ and $w_k^{b,1} = 0.005$ for $k \neq 1$. The values of $u_k^{b,1}$ and $v_k^{b,1}$ are discussed in more detail later.

The maximum number of hypotheses of the BG-TPMB filters is $N_h = 200$, the pruning threshold for

PPP weight is $\Gamma_P = 10^{-5}$, the pruning threshold for MB components is $\Gamma_{mb} = 10^{-5}$, and $L = 5$. The performance of the proposed filters is measured by the root mean square (RMS) $d(\cdot)$ of the trajectories set, i.e

$$d(k) = \sqrt{\frac{1}{N_{mc}k}\sum_{i=1}^{N_{mc}} d^2\left(\bar{\mathbf{X}}_k, \hat{\bar{\mathbf{X}}}_k^i\right)},$$

where $d(\cdot,\cdot)$ is the linear programming metric with $p = 2, c = 10$, and $\gamma = 1$; N_{mc} is the number of Monte Carlo runs; k indicates the time step(García-Fernández et al., 2020a).

5.1 Scenario 1

Five different initial beta parameters are set to verify the influence of initial beta parameters on the TPMB filters. Five different initial parameters of the beta distribution are set to $u = [9, 8, 7, 6, 5]$ and $v = [1, 2, 3, 4, 5]$, respectively. Finally, the detection probability of the sensor $p_D = 0.9$ and p_D doesn't change over time, $N_s = 81$ is the total time step, and $N_{mc} = 100$.

Figure 2 shows the detection probability estimates of TPMB for all trajectories under different beta parameters. In Fig.2, Truth represents the true trajectory detection probability and the true detection probability is $p_D = 0.9$, 9-1-TPMB represents the BG-TPMB filter for all trajectories with initial beta parameters $u = 9, v = 1$. It can be seen from Figure 2 that the filter proposed in this paper can effectively estimate the detection probability. The initial beta parameters are related to the rate at which the sensor's trajectory detection probability converges to the true detection probability. The closer the initial beta parameter is to the detection probability of the sensor, the faster the detection probability converges to the true probability of the sensor.

Figure 3 shows the trajectory metric error of the TPMB filter for all trajectories in different initial beta parameters, where standard-TPMB represents the TPMB filter that gives the detection probability as prior information, and Figure 4 is the decomposition of the trajectory metric error. It can be seen from Figures 3 and 4 that in the first 41 time steps, the trajectory error is inversely correlated with the initial detection probability and the initial parameter of the beta distribution; that is, the initial detection probability is approximately close to the true detection probability, and the error is smaller. After the time step of 41, the error is positively correlated with the initial detection probability. In addition, when the trajectory disappears, the error increases. This is due to the slow iteration of beta parameters, which leads to a delay in determining whether the trajectory has disappeared.

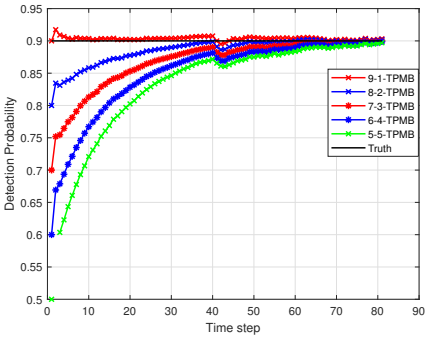

Fig. 2 Estimation of detection probability under different beta parameters for all trajectories

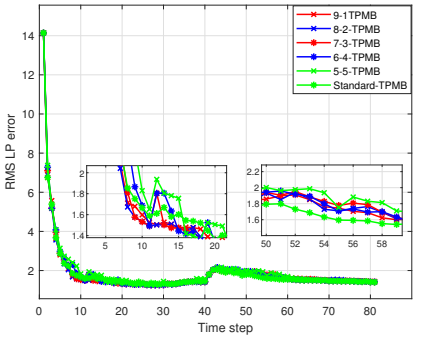

Fig. 3 Trajectory metric error for the all trajectories

The performance of the proposed filter is further analyzed by setting different clutter rates and detection probabilities. Given that the detection probabilities are set at $p_D = 0.9$ and 0.85, and the closer the initial beta parameter is to the true value of the detection probability, the smaller the error. Therefore, the initial beta distribution parameters are set to $u = 8$ and $v = 2$ for BG-TPMB and BG-TPHD.

Moreover, the clutter rate is set to three different values, $\bar{\lambda}_C = 10$, 20, and 30. The detection probability of standard PMB is set as above. Tables 1 and 2 show the resulting RMS error considering all

Table 1 Comparison of filter performance under different detection probability and clutter rate (all trajectories)

(p_D, λ)	BG-TPMB					TPMB				
	Tot	Loc	Fal	Mis	Switch	Tot	Loc	False	Mis	Switch
(0.9, 10)	2.45	1.40	0.68	1.88	0.21	2.45	1.39	0.56	1.93	0.22
(0.9, 20)	2.62	1.41	0.81	2.04	0.22	2.62	1.41	0.73	2.08	0.22
(0.9, 30)	2.82	1.45	1.08	2.15	0.21	2.74	1.44	0.81	2.18	0.21
(0.85, 10)	2.67	1.46	0.70	2.11	0.22	2.68	1.47	0.64	2.13	0.22
(0.85, 20)	2.90	1.51	0.91	2.29	0.21	2.90	1.50	0.84	2.33	0.21
(0.85, 30)	3.17	1.51	1.25	2.48	0.22	3.09	1.50	0.97	2.52	0.21

BG: beta-Gaussian; TPMB: trajectory Poisson multi-Bernoulli

Table 2 Comparison of filter performance under different detection probability and clutter rate (alive trajectories)

(p_D, λ)	BG-TPMB					TPMB					BG-TPHD				
	Total	Loc	Fal	Mis	Switch	Tot	Loc	False	Mis	Switch	Total	Loc	Fal	Mis	Switch
(0.9, 10)	5.43	1.82	3.47	3.74	0.18	5.58	1.84	3.51	3.93	0.18	7.37	1.93	3.78	6.03	0.19
(0.9, 20)	5.55	1.85	3.53	3.86	0.18	5.69	1.86	3.57	4.02	0.18	7.61	1.94	3.84	6.28	0.18
(0.9, 30)	5.55	1.85	3.56	3.84	0.18	5.69	1.86	3.54	4.04	0.18	7.74	1.95	3.93	6.37	0.19
(0.85, 10)	5.54	1.87	3.51	3.85	0.18	5.55	1.88	3.49	3.87	0.18	7.77	1.95	3.78	6.50	0.19
(0.85, 20)	5.68	1.91	3.56	3.99	0.17	5.66	1.90	3.51	4.00	0.17	8.07	1.98	3.92	6.77	0.18
(0.85, 30)	5.72	1.88	3.61	4.02	0.18	5.73	1.88	3.56	4.07	0.18	8.41	2.04	7.08	4.05	0.18

BG: beta-Gaussian; TPHD: trajectory PHD; TPMB: trajectory Poisson multi-Bernoulli

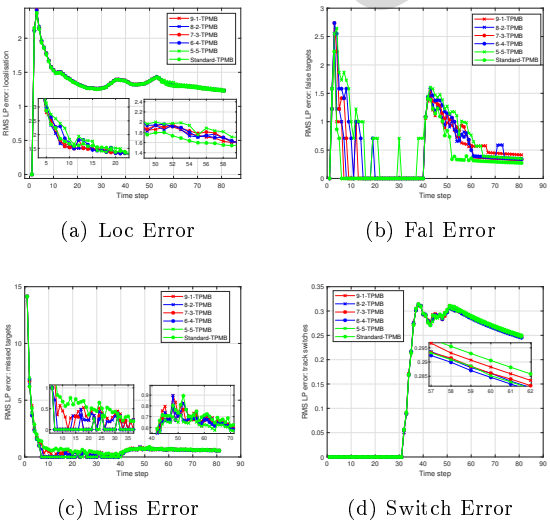

(a) Loc Error (b) Fal Error

(c) Miss Error (d) Switch Error

Fig. 4 Decomposition of trajectory metric error for the all trajectories

time steps, where the errors are calculated as follows:

$$d_T = \sqrt{\frac{1}{N_s}\sum_{i=1}^{N_s} d^2(k)}.$$

From Table 1, it can be seen that in the case of unknown sensor detection probability, the performance of the filter proposed in this paper is not significantly different from the standard TPMB. This indicates that the proposed filter in this paper is able to effectively estimate the target position when the detection probability is unknown.

As shown in Table 2, as the clutter Poisson rate increases, the errors of each filter also increase. With the same detection probability and clutter Poisson rate, the total error of the BG-TPMB algorithm is the smallest, while the BG-TPHD filter has the largest error. The overall error of the BG-TPMB algorithm is higher than that of the standard TPMB filter. However, in terms of false detection error, the standard TPMB filter outperforms the BG-TPMB filter.

The average running times of one MC in sec-

onds are: 1.18(BG-TPMB) and 0.64(BG-TPHD). It can be seen that the proposed BG-TPMB filter has better performance than BG-TPHD, but its computational cost is higher. This is always the case with standard TPMB and standard TPHD.

5.2 Scenario 2

In scenario 1, the detection probability is fixed throughout the process, while the sensor tends to reduce the detection probability as the continuous working time becomes longer in actual work. In this section, the detection probability is set as follows:

$$P_d(k) = \begin{cases} 0.9, & k \leq 41; \\ 0.8, & k > 41. \end{cases}$$

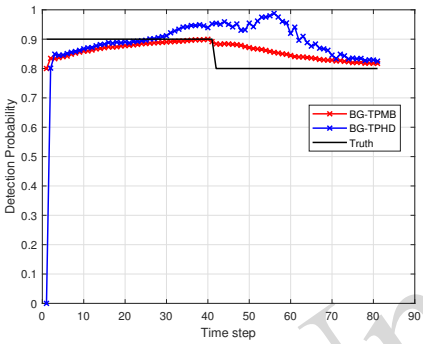

Fig. 5 Estimation of detection probability for alive trajectories

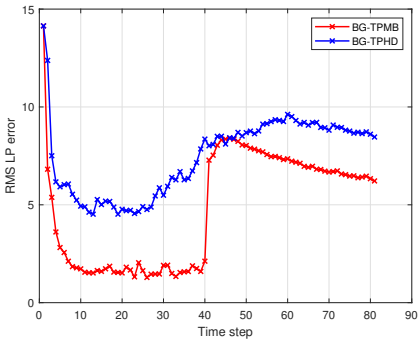

Fig. 6 Trajectory metric error for alive trajectories

The initial beta function parameters are set as $u = 8, v = 2$. The clutter rate is $\bar{\lambda}_C = 10$. Finally, the error of the set of alive trajectories is compared with the TPHD filter. The results are shown in Figures 5-7. The reason for not comparing all trajectories with the TPHD filter is that the TPHD filter does not handle this problem.

Compared to the BG-TPHD filter, the proposed BG-TPMB filter for alive trajectory demonstrates better performance, greater sensitivity to abrupt changes in detection probability, and improved accuracy in estimating detection probability. The trajectory error increases after time step 41. At step 41, the detection probability and the number of trajectories change simultaneously. The change in the sensor detection probability leads to the change in the measurements generated by the trajectories and the presence of clutter in the scene, so the dead trajectory may still be regarded as alive, and the wrong association between the trajectories and clutter leads to the increase of errors at step 41. It is worth noting that the proposed filter error increases when a trace disappears, which is consistent with the case of the standard TPMB filter for alive trajectories.

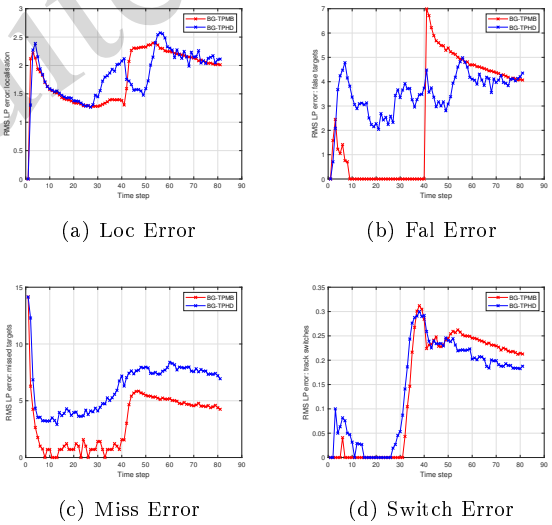

(a) Loc Error (b) Fal Error

(c) Miss Error (d) Switch Error

Fig. 7 Decomposition of trajectory metric error for alive trajectories

The performance of the proposed filter is further analyzed by setting different detection probabilities for each trajectory. The detection probability of trajectory 1 is 0.95, that of trajectory 2 is 0.9, and that of trajectory 3 and trajectory 4 is 0.8. Moreover, the detection probability of standard TPMB is set as 0.95 and the initial beta function parameters are set as $u = 8, v = 2$.

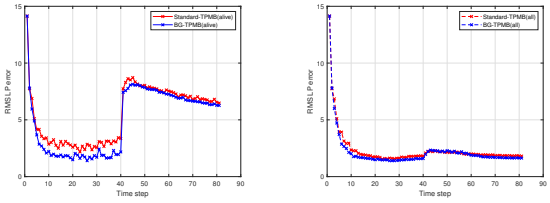

(a) All trajectories Error (b) Alive trajectories Error

Fig. 8 Trajectory metric error of different detection probabilities for each trajectory

As can be seen from Fig.8, the filters proposed in this paper can still maintain effective tracking in the face of different detection probabilities of each trajectory. Compared with the standard TPMB given as prior information with fixed detection probabilities, the filters proposed in this paper have better tracking performance.

6 Conclusion

This paper proposes two trajectory filters that perform robustly when the detection probability is unknown. These TPMB filters are implemented using the BG mixture method, known as BG-TPMB filters. Specifically, the Poisson intensity is approximated as a BG mixture form, and the spatial probability density of Bernoulli components is approximated as a single BG form. Furthermore, the detailed recursive solutions are derived for TPMB filters with unknown detection probability and closed-forms for the BG implementation of both alive trajectories and all trajectories are given. Finally, simulation results demonstrate that the proposed TPMB filters in this paper can adjust to the unknown detection probability and changes in detection over time.

Contributors

Xiangfei ZHENG designed the research. Xiangfei ZHENG and Hongwei LI processed the data. Xiangfei ZHENG drafted the paper. Kaidi LIU and Hongwei LI helped organize the paper. Xiangfei ZHENG , Kaidi LIU, and Hongwei LI revised and finalized the paper.

Conflict of interest

All the authors declare that they have no conflict of interest.

References

Bishop CM, 2006. Pattern Recognition and Machine Learning. Springer, New York, USA.

Blackman SS, 2004. Multiple hypothesis tracking for multiple target tracking. *IEEE Aerosp Electron Syst Mag*, 19(1):5-18. https://doi.org/10.1109/MAES.2004.1263228

Chen TT, Wang RL, Dai B, et al., 2016. Likelihood-field-model-based dynamic vehicle detection and tracking for self-driving. *IEEE Trans Intell Transport Syst*, 17(11):3142-3158. https://doi.org/10.1109/TITS.2016.2542258

Fortmann T, Bar-Shalom Y, Scheffe M, 1983. Sonar tracking of multiple targets using joint probabilistic data association. *IEEE J Oceanic Eng*, 8(3):173-184. https://doi.org/10.1109/JOE.1983.1145560

Gao L, Battistelli G, Chisci L, 2020. Random finite set based distributed multirobot slam. *IEEE Trans Robot*, 36(6):1758-1777. https://doi.org/10.1109/TRO.2020.3001664

García-Fernández ÁF, Svensson L, 2019. Trajectory phd and cphd filters. *IEEE Trans Signal Process*, 67(22):5702-5714. https://doi.org/10.1109/TSP.2019.2943234

García-Fernández ÁF, Williams JL, Granström K, et al., 2018. Poisson multi-bernoulli mixture filter: Direct derivation and implementation. *IEEE Trans Aerosp Electron Syst*, 54(4):1883-1901. https://doi.org/10.1109/TAES.2018.2805153

García-Fernández ÁF, Rahmathullah AS, Svensson L, 2020a. A metric on the space of finite sets of trajectories for evaluation of multi-target tracking algorithms. *IEEE Trans Signal Process*, 68:3917-3928. https://doi.org/10.1109/TSP.2020.3005309

García-Fernández ÁF, Svensson L, Morelande MR, 2020b. Multiple target tracking based on sets of trajectories. *IEEE Trans Aerosp Electron Syst*, 56(3):1685-1707. https://doi.org/10.1109/TAES.2019.2921210

García-Fernández ÁF, Svensson L, Williams JL, et al., 2020c. Trajectory poisson multi-bernoulli filters. *IEEE Trans Signal Process*, 68:4933-4945. https://doi.org/10.1109/TSP.2020.3017046

Granström K, Natale A, Braca P, et al., 2015. Gamma gaussian inverse wishart probability hypothesis density for extended target tracking using x-band marine radar data. *IEEE Trans Geosci Remote Sens*, 53(12):6617-6631. https://doi.org/10.1109/TGRS.2015.2444794

Granström K, Svensson L, Xia YX, et al., 2018. Poisson multi-bernoulli mixture trackers: Continuity through random finite sets of trajectories. Proc 21st Int Conf on Information Fusion, p.1-5. https://doi.org/10.23919/ICIF.2018.8455849

Granström K, Fatemi M, Svensson L, 2020. Poisson multi-bernoulli mixture conjugate prior for multiple extended target filtering. *IEEE Trans Aerosp Electron Syst*, 56(1):208-225. https://doi.org/10.1109/TAES.2019.2920220

Houssineau J, Zeng JJ, Jasra A, 2021. Uncertainty modelling and computational aspects of data association. *Stat Comput*, 31(5):59. https://doi.org/10.1007/s11222-021-10039-1

Joshi SK, Baumgartner SV, Krieger G, 2022. Tracking and track management of extended targets in range-doppler using range-compressed airborne radar data. *IEEE Trans Geosci Remote Sens*, 60:5102720. https://doi.org/10.1109/TGRS.2021.3084862

Li GC, Kong LJ, Yi W, et al., 2021. Robust poisson multi-bernoulli mixture filter with unknown detection probability. *IEEE Trans Veh Technol*, 70(1):886-899. https://doi.org/10.1109/TVT.2020.3047107

Li TC, Chen HM, Sun SD, et al., 2019. Joint smoothing and tracking based on continuous-time target trajectory function fitting. *IEEE Trans Automat Sci Eng*, 16(3):1476-1483. https://doi.org/10.1109/TASE.2018.2882641

Mahler RPS, Vo BT, Vo BN, 2011. Cphd filtering with unknown clutter rate and detection profile. *IEEE Trans Signal Process*, 59(8):3497-3513. https://doi.org/10.1109/TSP.2011.2128316

Mahler RPS, 2007. Statistical multisource-multitarget information fusion. Artech House, Boston,USA.

Mahler RPS, 2014. Advances in statistical multisource-multitarget information fusion. Artech House, Boston,USA.

Menegaz HMT, Battistini S, 2018. Switching multiple model filter for boost-phase missile tracking. *IEEE Trans Aerosp Electron Syst*, 54(5):2547-2553. https://doi.org/10.1109/TAES.2018.2822118

Pang S, Morris D, Radha H, 2021. 3d multi-object tracking using random finite set-based multiple measurement models filtering (rfs-m3) for autonomous vehicles. Proc IEEE Int Conf on Robotics and Automation, p.13701-13707. https://doi.org/10.1109/ICRA48506.2021.9561852

Vo BN, Ma WK, 2006. The gaussian mixture probability hypothesis density filter. *IEEE Trans Signal Process*, 54(11):4091-4104. https://doi.org/10.1109/TSP.2006.881190

Vo BN, Vo BT, Phung D, 2014. Labeled random finite sets and the bayes multi-target tracking filter. *IEEE Trans Signal Process*, 62(24):6554-6567. https://doi.org/10.1109/TSP.2014.2364014

Vo BT, Vo BN, 2013. Labeled random finite sets and multi-object conjugate priors. *IEEE Trans Signal Process*, 61(13):3460-3475. https://doi.org/10.1109/TSP.2013.2259822

Vo BT, Vo BN, Cantoni A, 2007. Analytic implementations of the cardinalized probability hypothesis density filter. *IEEE Trans Signal Process*, 55(7):3553-3567. https://doi.org/10.1109/TSP.2007.894241

Vo BT, Vo BN, Cantoni A, 2009. The cardinality balanced multi-target multi-bernoulli filter and its implementations. *IEEE Trans Signal Process*, 57(2):409-423. https://doi.org/10.1109/TSP.2008.2007924

Vo BT, Vo BN, Hoseinnezhad R, et al., 2013. Robust multi-bernoulli filtering. *IEEE J Sel Top Signal Process*, 7(3):399-409. https://doi.org/10.1109/JSTSP.2013.2252325

Wei SX, Zhang BX, Yi W, 2022. Trajectory phd and cphd filters with unknown detection profile. *IEEE Trans Veh Technol*, 71(8):8042-8058. https://doi.org/10.1109/TVT.2022.3174055

Wu SY, Zhou YS, Xie Y, et al., 2022. Robust poisson multi-bernoulli mixture filter using adaptive birth distributions for extended targets. *Digital Signal Process*, 126:103459. https://doi.org/10.1016/j.dsp.2022.103459

Xia YX, Granström K, Svensson L, et al., 2022. Poisson multi-bernoulli approximations for multiple extended object filtering. *IEEE Trans Aerosp Electron Syst*, 58(2):890-906. https://doi.org/10.1109/TAES.2021.3111720

Xie XX, Wang Y, Guo JQ, et al., 2023. Pmbm filter for multiple extended targets with unknown clutter rate and detection probability. *IEEE Sensors J*, 23(15):17133-17147. https://doi.org/10.1109/JSEN.2023.3285885

Yan B, Paolini E, Xu LP, et al., 2022. A target detection and tracking method for multiple radar systems. *IEEE Trans Geosci Remote Sens*, 60:5114721. https://doi.org/10.1109/TGRS.2022.3183387

Yu M, Gong LY, Oh H, et al., 2018. Multiple model ballistic missile tracking with state-dependent transitions and gaussian particle filtering. *IEEE Trans Aerosp Electron Syst*, 54(3):1066-1081. https://doi.org/10.1109/TAES.2017.2773258

List of electronic supplementary materials

SM1 Proof of proposition 1

SM2 Proof of proposition 2

SM3 Beta Gaussian mixture merging